CHAPTER 4

RESULTS

PART A : Zn(II)-NH_3 Intermolecular Potential

4.1 Zn(II)-NH_3 Intermolecular Pair Potential

After having calculated 575 Zn(II)-NH_3 SCF energy points, the interaction energies were fitted to the analytical form

$$\Delta E(r) = \sum_{i=1}^{4} A_i / r_i^3 + B_i / r_i^4 + C_i \exp(-D_i r_i) + 332.15\, q_i q_{Zn(II)} / r_i$$

where r_i is the distance between the i-th atom of ammonia and Zn(II). q_i and $q_{Zn(II)}$ are the net charges of the i-th atom of ammonia and of Zn(II), respectively. The parameters are given in Table 4.1, the standard deviations between SCF data and fitted data in table 4.2. The stabilization energies obtained from the quantum chemical calculations ΔE_{SCF} are plotted versus those obtained from the function ΔE_{FIT} in Fig. 4.1 and their variations as a function of Zn(II)-N distance are exhibited in Fig. 4.2 .

Table 4.1 Final optimized parameters for the interaction of H and N atoms of ammonia with Zn(II). Interaction energies and r in kcal/mol and Å, respectively.

Atom	q	A	B	C	D
N	-0.83433	-.1550601E+04	.1173522E+04	.4021063E+05	.3374070E+01
H	0.27811	.1763222E+03	-.8160192E+02	.1501402E+02	.4323704E+00

Table 4.2 Number of SCF-data points (*N*) and standard deviation (σ in kcal/mol) of the fitting for Zn(II)-NH_3 interactions.

N	σ
475	0.411
575	0.409

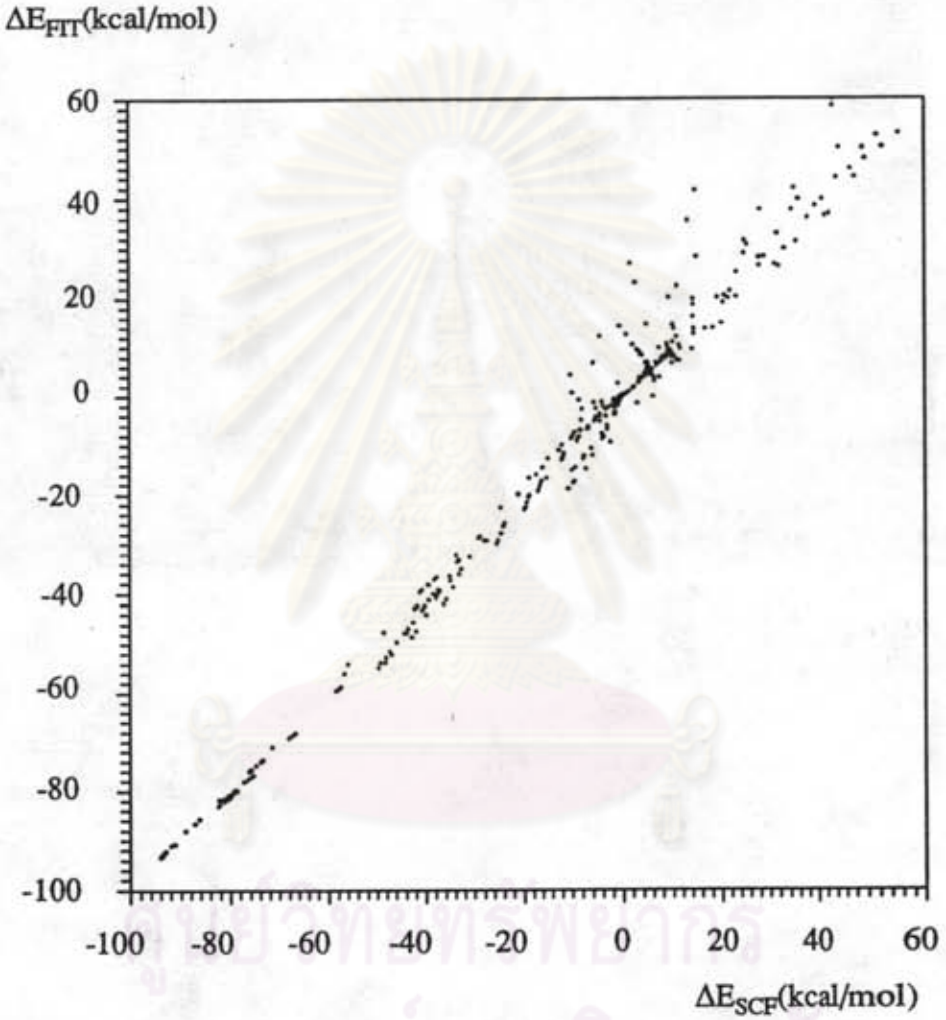

Fig 4.1 Comparison of the stabilization energies from the SCF calculations (ΔE_{SCF}) and the potential function using the final values of the fitting parameters as given in Table 4.1 (ΔE_{FIT}).

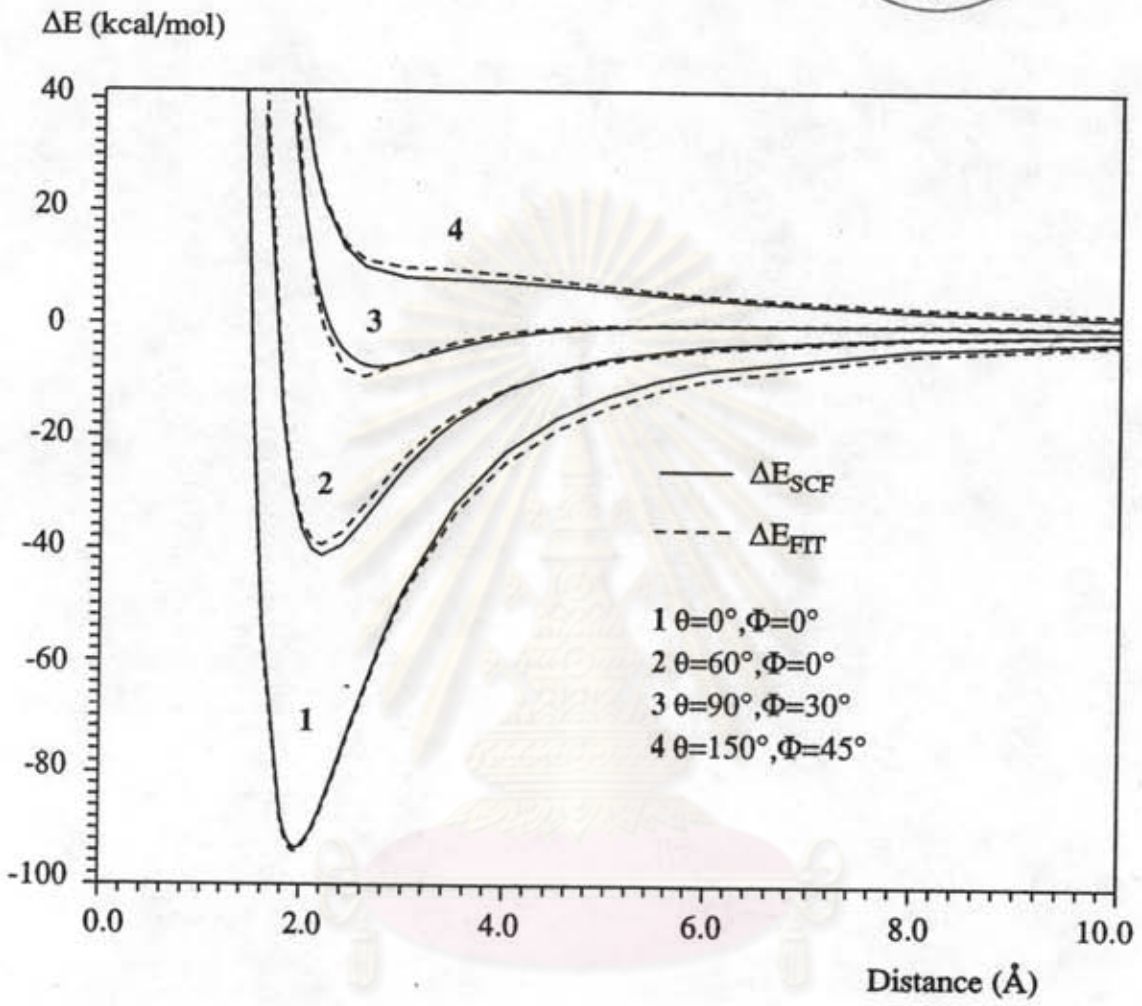

Fig 4.2 Comparison of the stabilization energies obtained from SCF calculations and potential function.

4.2 Zn(II)-NH_3 Intermolecular Potential with Three-body Correction

4.2.1 Non-Additivity of Zn(II)-NH_3 Pair Potential

The resulting values for ΔE_{av1} and ΔE_{2FCN} (see 2.5.2) are summarized in Table 4.3, together with the ligand-ligand repulsion energies, ΔE_{rpl}, and the

corresponding percentage of non-additivity, $\%E_1$ and $\%E_2$, defined by:

$$\%E_1 = 100(1 - \Delta E_{av1}^{n=1} / \Delta E_{av1}^{n\neq1})$$

$$\%E_2 = 100(1 - \Delta E_{av1} / \Delta E_{2FCN})$$

$$\Delta E_{rpl} = E[L_n] - nE[L]$$

Table 4.3 Interaction energies and optimized ion-nitrogen distances (r_{M-N}) for different Zn(II)-$(NH_3)_n$ complexes (energies in kcal/mol and r in Å).

n	r_{M-N}	ΔE_{av1}	$\%E_1$	ΔE_{2FCN}	$\%E_2$	ΔE_{rpl}
1	1.95	-94.07	0	-94.04	0	0.0
2	1.96	-92.48	2	-94.08	2	4.0
3	2.03	-86.91	8	-93.22	7	14.2
4	2.11	-80.56	14	-90.17	11	26.1
6	2.28	-68.03	28	-83.32	18	65.0

4.2.2 Three-body terms

After having calculated more than 1,500 configurations of the Zn(II)-$(NH_3)_2$ system and 4,500 Zn(II)-NH_3 and NH_3-NH_3 energy points, the interaction

energies were fitted to the analytical form

$$\Delta E_{3bd} = A \exp(-B(r_1 + r_2) - Cr_3)$$

where A, B, and C are adjustable parameters. The optimized parameters are given in Table 4.4 . r_1 and r_2 are the distances between Zn(II) and the nitrogen atoms of the two ammonia molecules, r_3 is distance between the nitrogens of the ammonia molecules, as shown in Fig 4.3 .

Table 4.4 Final optimized parameters of the three-body correction terms (standard deviation of the fitting = 0.739 kcal/mol)

A (kcal/mol)	B ($Å^{-1}$)	C ($Å^{-1}$)
547.90577	0.48477295	0.66989036

In order to investigate in more detail the dependence of the three-body correction function on variables r_1 and r_2, three-dimensional ΔE_{3bd} plots were produced in Fig. 4.4 (a)- 4.4(d). Zn(II) is placed at the origin of the coordinate system, the nitrogen atom of the first ammonia molecule is fixed in the positive x-axis at characteristic values of r_1(Zn(II)-N_1 distance), pointing with its dipole moment vector towards Zn(II). The nitrogen atom of the second ammonia molecule is moved along radial lines around Zn(II) in the xy-plane, pointing with its dipole vector to the metal ion. Fig. 4.4 (a)- 4.4

(d) show the surface for r_1 = 1.95 Å, 2.0 Å, 3.0 Å and 5.0 Å, respectively.

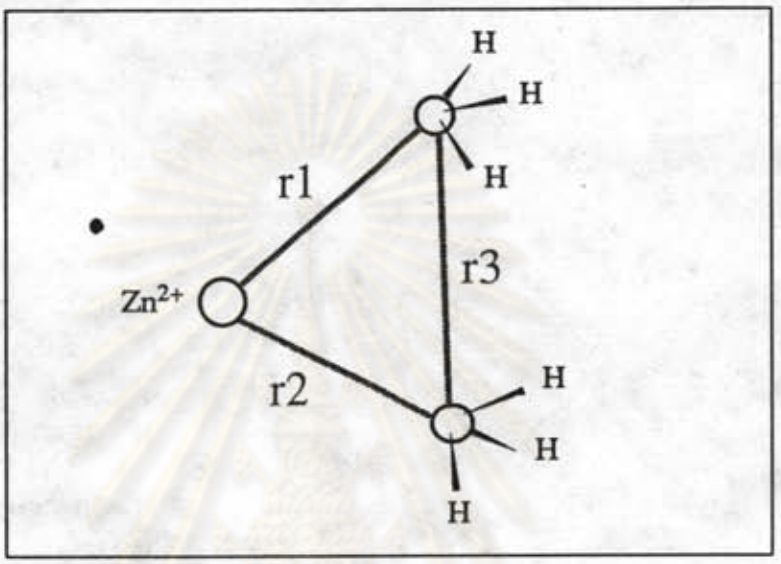

Fig 4.3 Definition of r_1, r_2, and r_3 of Zn(II)-$(NH_3)_2$

Fig 4.4 Potential surfaces for 3-body effect in the Zn(II)-$(NH_3)_2$ complex as a function of ligand locations (details see text)

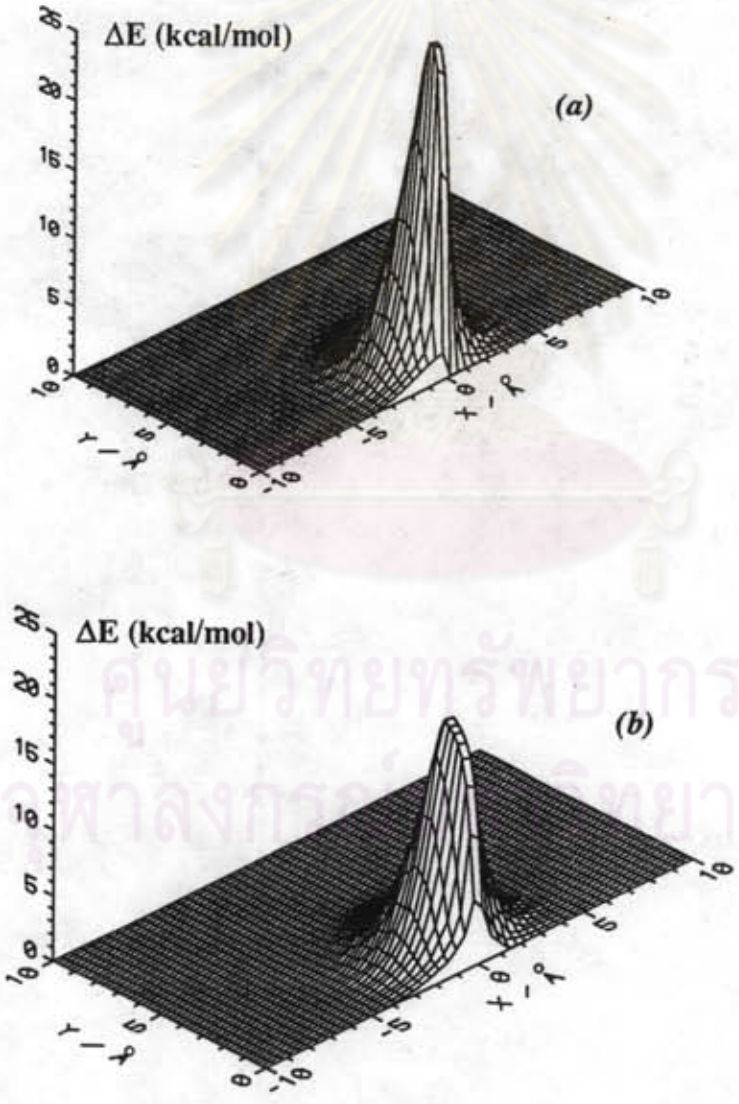

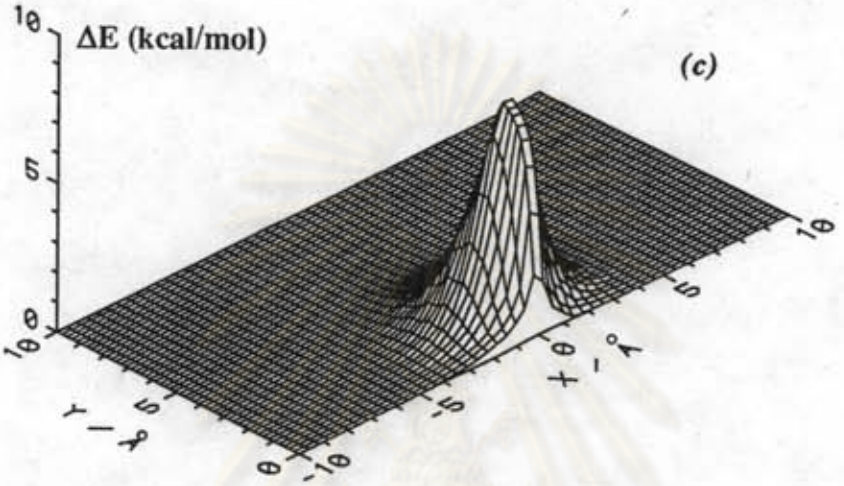
ΔE (kcal/mol)
(c)
10
5
0
10
5
0
-5
-10
Y
X

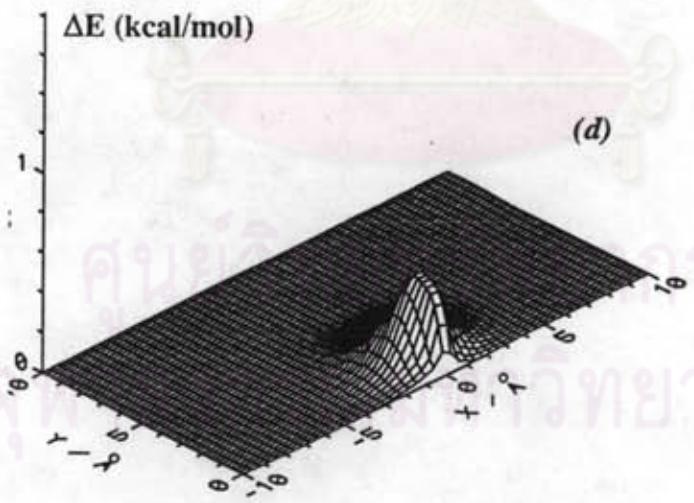
ΔE (kcal/mol)
(d)
1
0.0
10
5
0
-5
-10
Y
X

4.2.3 Monte Carlo Simulations : Radial Distribution Functions and Running Integration Numbers

To evaluate the effect of the three-body correction, Monte Carlo simulations were performed using the intermolecular pair potentail without and including three-body correction function. The Zn(II)-N radial distribution functions and running integration numbers of both runs are shown in Fig. 4.5 .

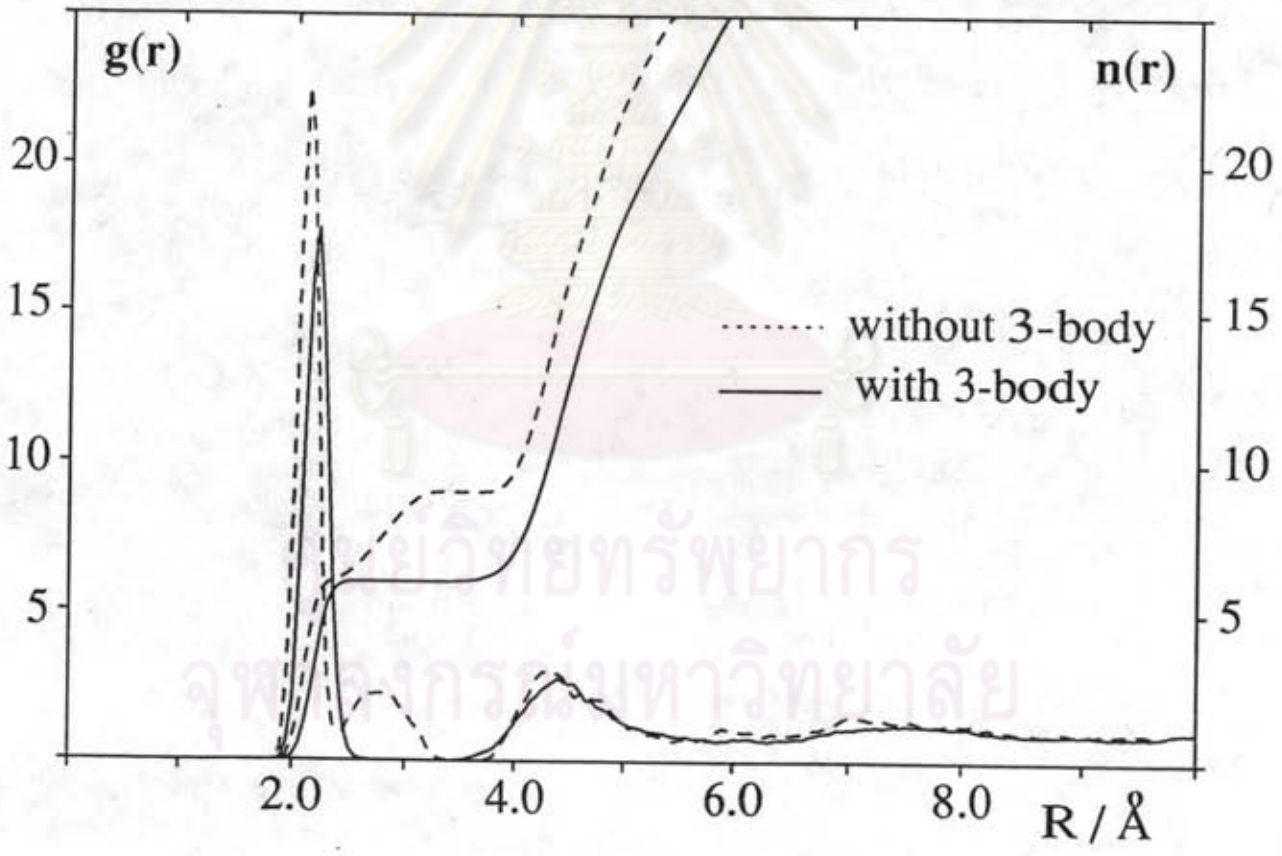

Fig 4.5 Zn(II)-N radial distribution functions and corresponding running integration numbers from Monte Carlo simulations with and without three-body corrections.

4.3 Molecular Dynamics Simulation using Zn(II)-NH_3 Intermolecular Pair Potential without Three-body Correction

Molecular Dynamics simulations at 235 K and 266 K of the system using the Zn(II)-NH_3 intermolecular pair potential without three-body correction were performed in order to evaluate radial distribution functions and running integration numbers (Fig. 4.6).

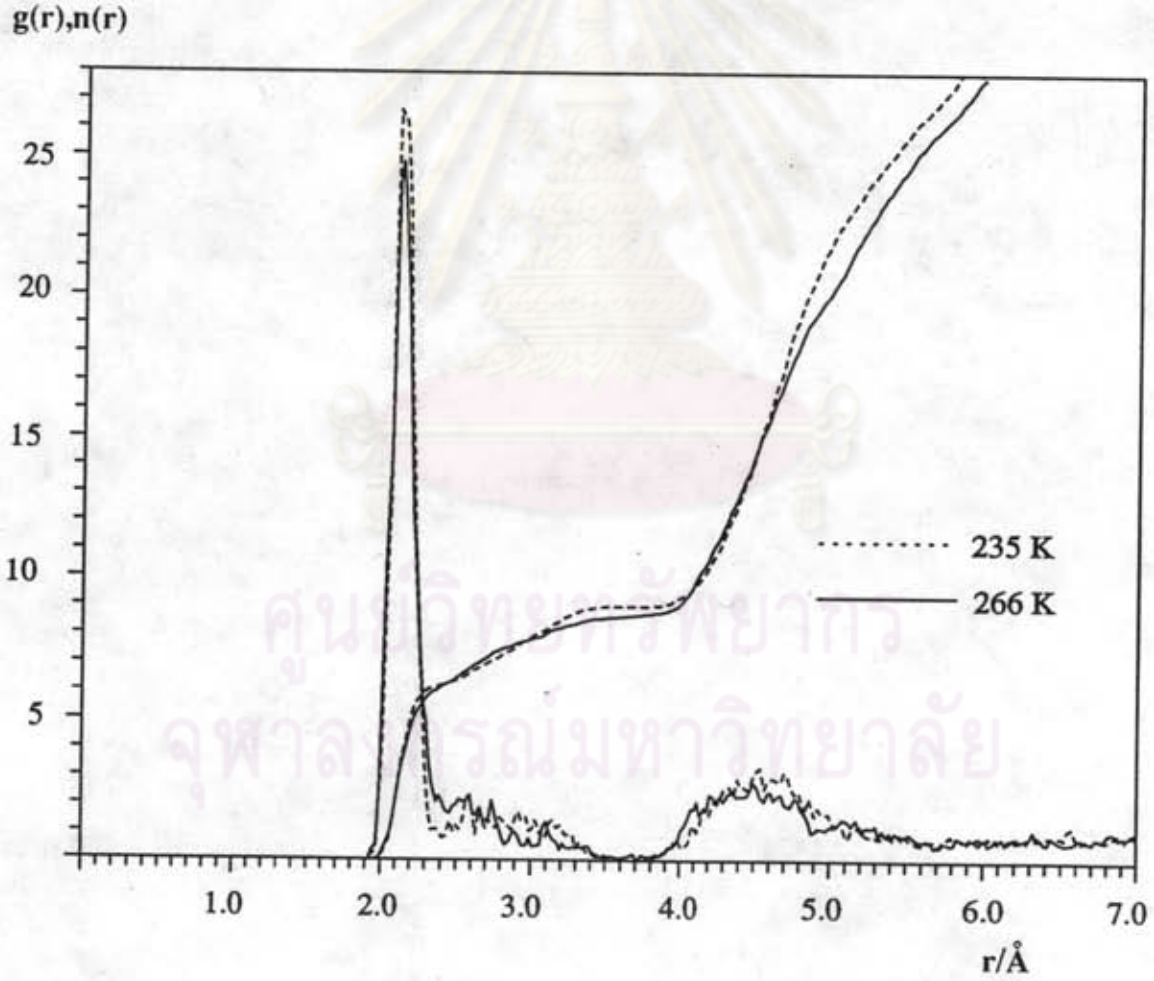

Fig. 4.6 Zn(II)-N radial distribution functions and corresponding running integration numbers from Molecular Dynamics simulations at 235 K and 266 K.

PART B : Molecular Dynamics Simulation of a Zn(II) in Liquid Ammonia with Three-body Correction

4.4 Static Properties

4.4.1 Solution Structure

The solution structure of this study are reported in terms of radial distribution functions, $g_{\alpha\beta}(r)$, and running integration numbers, $n_{\alpha\beta}(r)$. Table 4.5 shows some important values, especially the first maximum and mimimum, of the radial distribution functions of the Zn(II)-ammonia solution in comparison with NN and ZnO radial distribution functions from Narten [73] and Yongyai [74], respectively.

Zn(II)-N ,N-N and N-H, and H-H radial distribution functions and their corresponding running integration numbers are depicted in Fig. 4.7, 4.8 and 4.9, respectively.

Table 4.5 Characteristic values of the radial distribution functions $g_{\alpha\beta}(r)$ for the Zn(II)-NH_3 solution. r_{M1}, r_{M2} and r_{m1} are the distance in Å, where $g_{\alpha\beta}(r)$ has first and second maximum and first minimum, respectively.

αβ	T/K	r_{M1}	$g_{\alpha\beta}(r_{M1})$	r_{m1}	$g_{\alpha\beta}(r_{m1})$	$n_{\alpha\beta}(r_{m1})$	r_{M2}
NN	235	3.34	2.1	5.0	0.75	12.1	6.61
	266	3.32	2.0	5.0	0.79	12.0	6.57
NH	235	3.57	1.3	5.1	0.9	38.7	6.63
	266	3.77	1.3	5.2	0.9	38.7	6.81
HH	235	3.72	1.2	5.2	0.9	42.2	-
	266	3.77	1.2	5.2	0.9	39.8	-
ZnN	235	2.23	16.5	2.72	0.0	6.0	5.34
	266	2.21	18.8	2.68	0.0	6.0	4.83
ZnH	235	2.86	5.9	3.52	0.0	18.0	5.6
	266	2.88	8.4	3.43	0.0	18.0	5.2
NN[(a)]	277	3.37	2.1	5.0	0.75	12.0	6.9
ZnO[(b)]	298	2.05	23.8	2.2	0.0	6.0	-

(a) : experimental $g_{NN}(r)$ taken from reference [73]

(b) : Monte Carlo $g_{ZnO}(r)$ taken from reference [74]

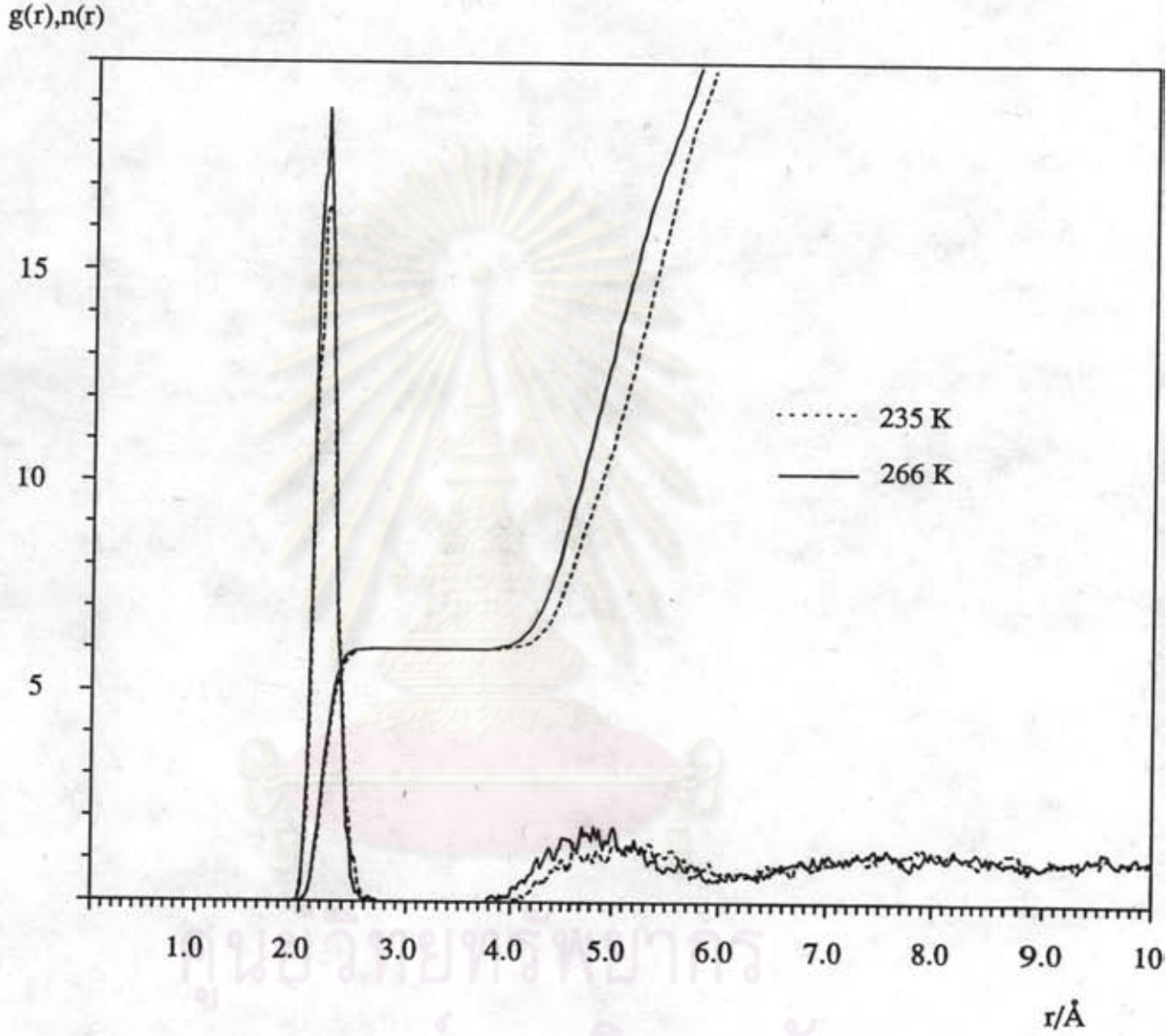

Fig. 4.7 Zn(II)-N radial distribution functions and running integration numbers at 235 K (dashed) and 266 K (solid).

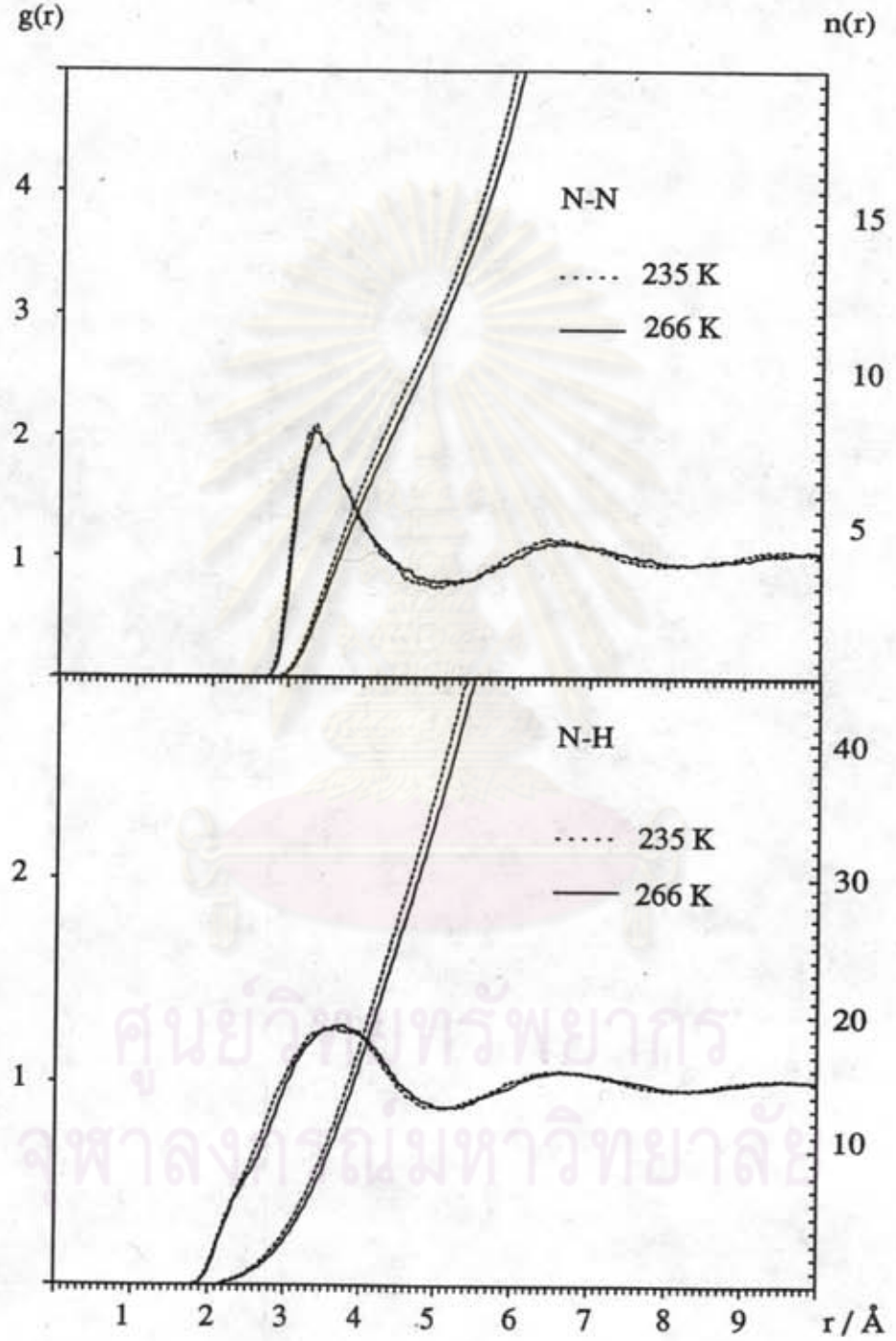

Fig 4.8 N-N and N-H radial distribution functions and running integration numbers at 235 K (dashed) and 266 K (solid).

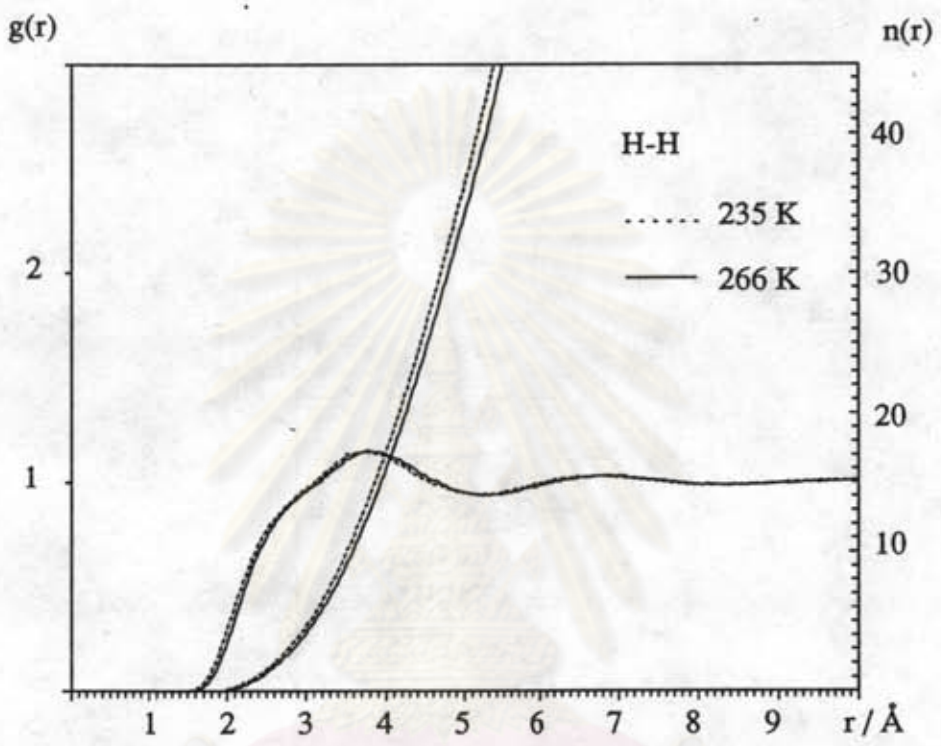

Fig 4.9 H-H radial distribution functions and running integration numbers at 235 K (dashed) and 266 K (solid).

4.4.2 Intramolecular Geometry

The flexible model for ammonia molecule permits the investigation of the effect of the cation on the molecular geometry. In Fig 4.10, Fig 4.11 and Fig 4.12 the distribution of the N-H distances, H-H distances and HNH angles are depicted, calculated separately for ammonia molecules in the bulk and in the first solvation shell of Zn(II).

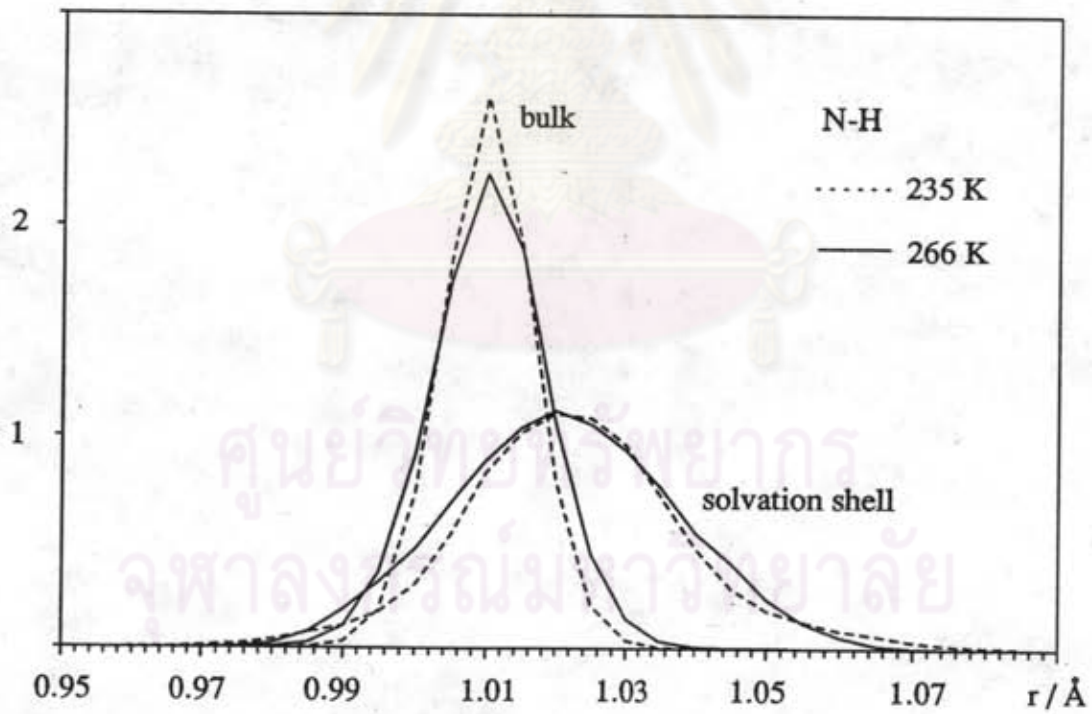

Fig 4.10 Normalized distributions of the intramolecular N-H distances in arbitrary units at 235 K (dashed) and 266 K (solid), calculated separately for ammonia molecules in the bulk and in the solvation shell of Zn(II).

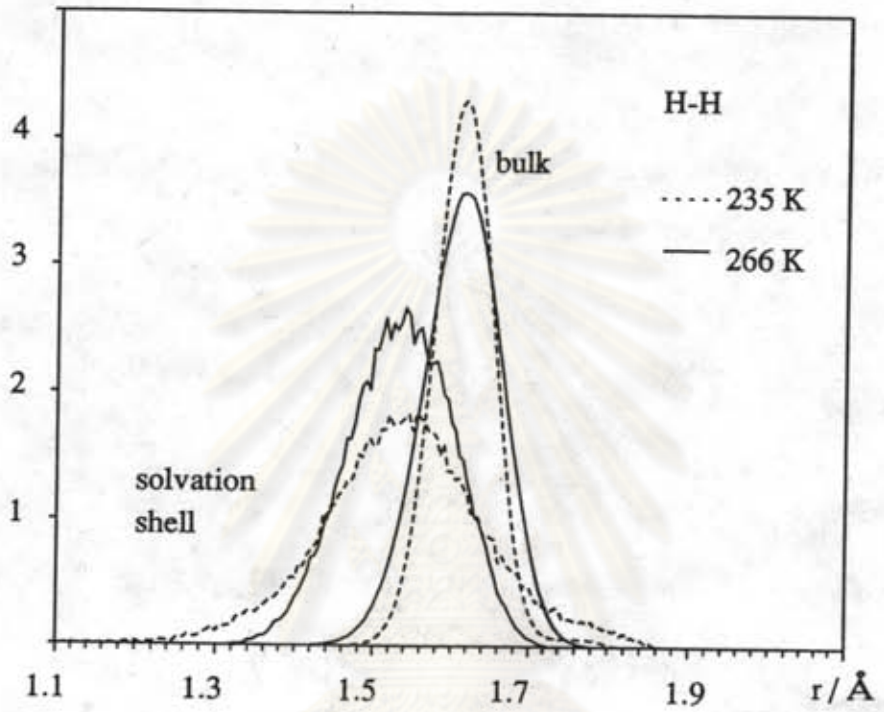

Fig 4.11 Normalized distribution of the intramolecular H-H distances in arbitrary units at 235 K (dashed) and 266 K (solid), calculated separately for ammonia molecules in the bulk and in the solvation shell of Zn(II).

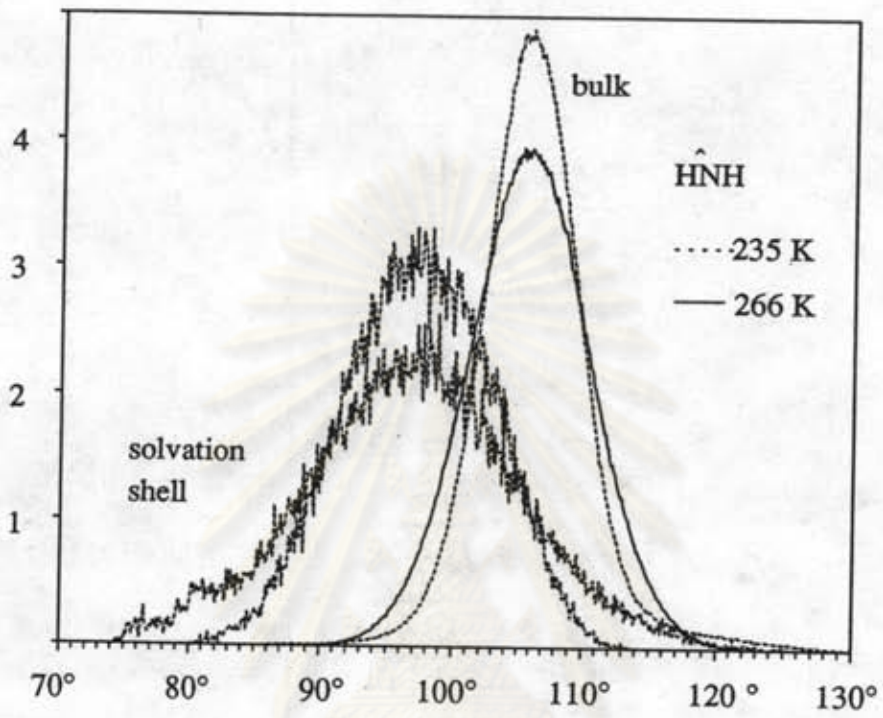

Fig. 4.12 Normalized distributions of the intramolecular HNH angles in arbitrary units at 235 K (dashed) and 266 K (solid), calculated separately for ammonia molecules in the bulk and in the solvation shell of Zn(II).

4.5 Dynamic Properties

Dynamic properties of the Zn(II)-NH_3 solution are reported only for the velocity autocorrelation functions (ACFs or $C_v(t)$).

In Fig 4.13 normalized velocitiy autocorrelation function of Zn(II) is depicted. ACF of ammonia molecule, nitrogen atom and hydrogen atom are drawn in Fig. 4.14, Fig. 4.15 and Fig 4.16, respectively.

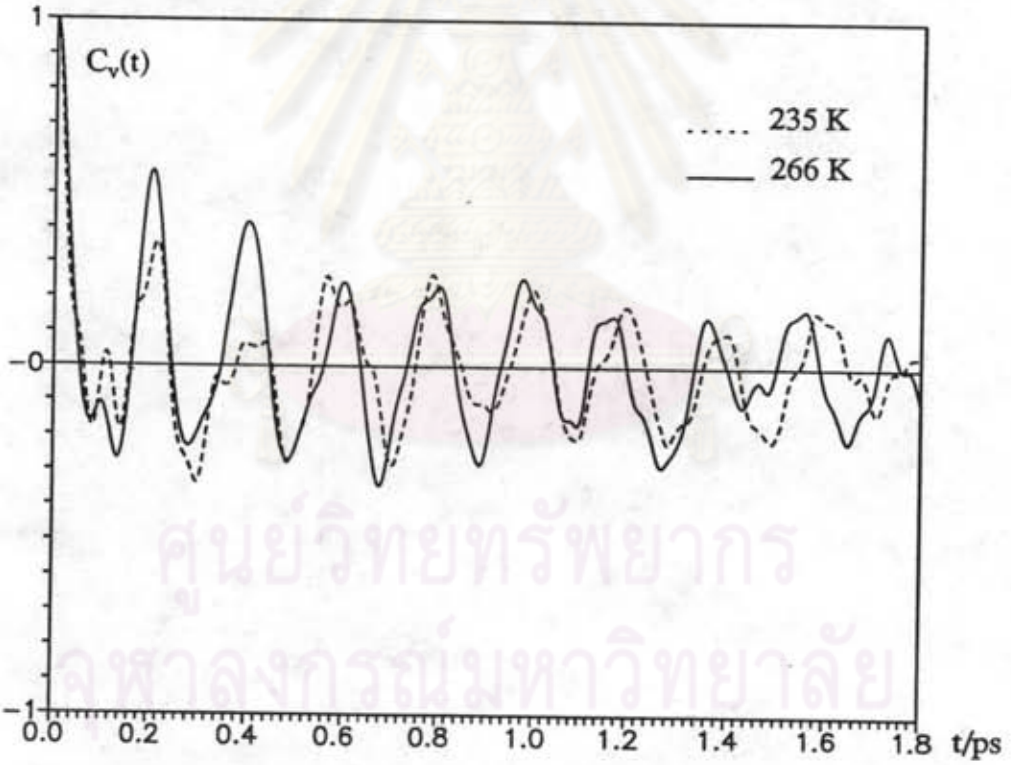

Fig. 4.13 Normalized velocity autocorrelation functions of Zn(II) at 235 K (dashed) and 266 K (solid).

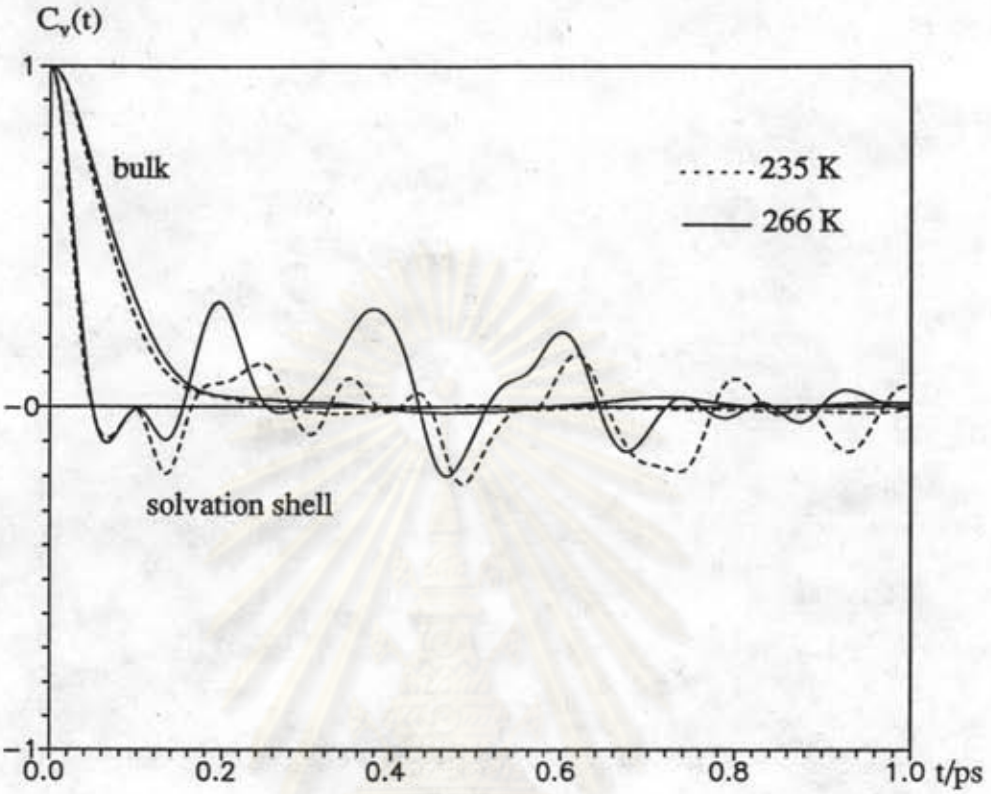

Fig. 4.14 Normalized center-of-mass velocity autocorrelation functions of ammonia molecules at 235 K (dashed) and 266 K (solid), calculated separately for bulk ammonia and ammonia in the solvation shell of Zn(II).

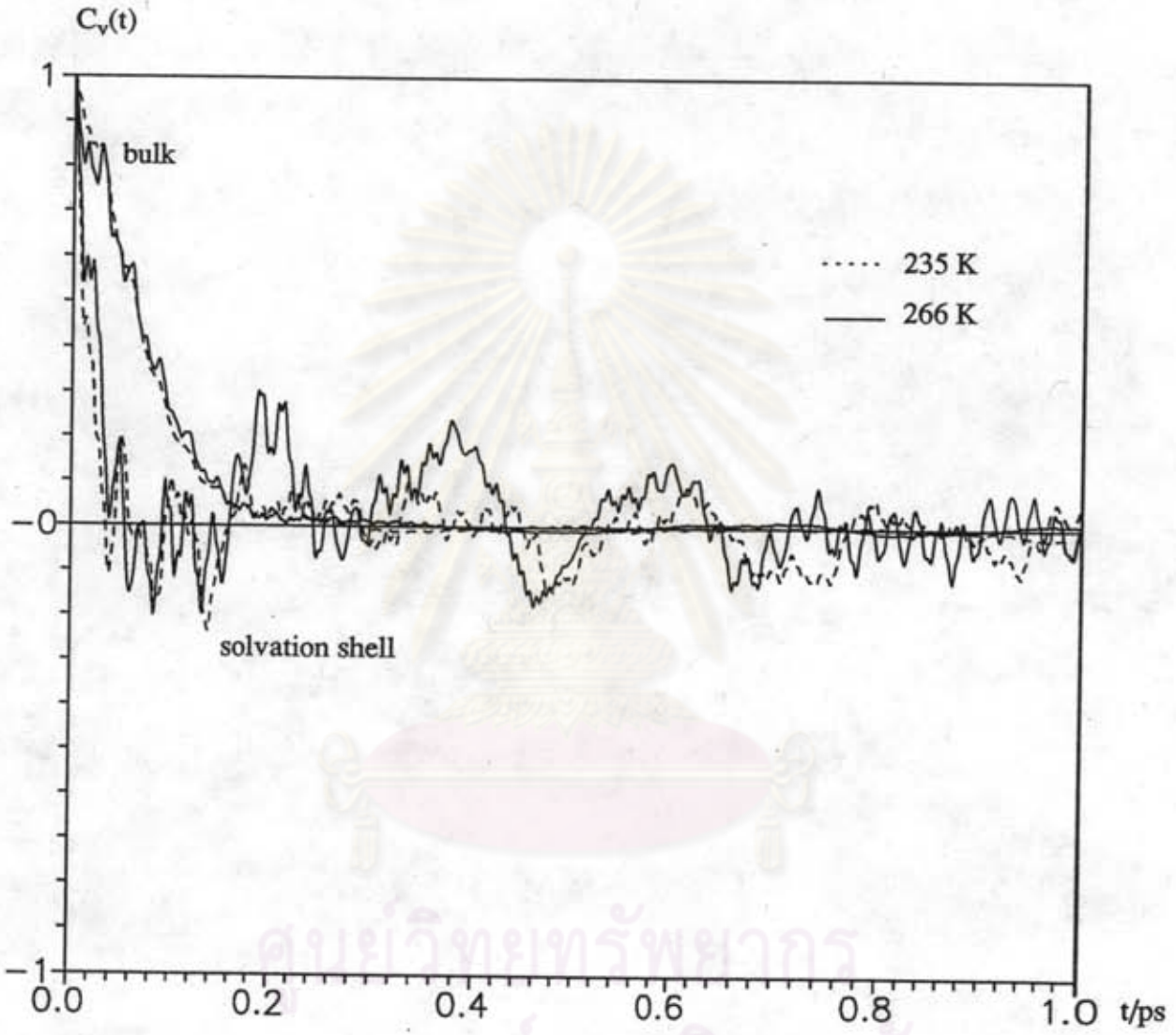

Fig 4.15 Normalized autocorrelation functions of nitrogen at 235 K (dashed) and 266 K (solid), calculated separately for ammonia molecules in the bulk and in the solvation shell of Zn(II).

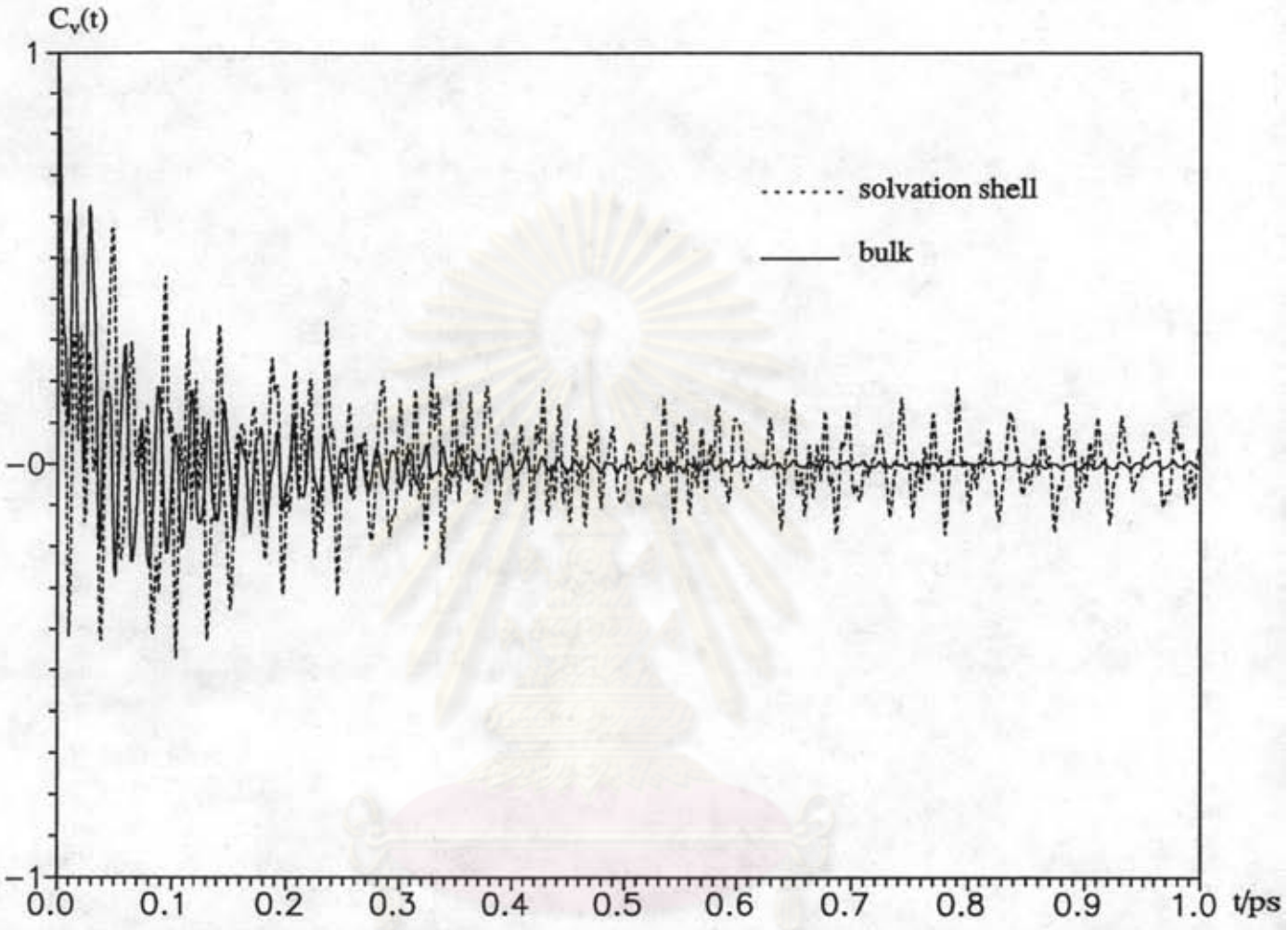

Fig 4.16 Normalized autocorrelation functions of hydrogen at 235 K, calculated separately for ammonia molecules in the bulk and in the solvation shell of Zn(II).